International Journal of Minerals, Metallurgy and Materials
Volume 29, Number 8, August 2022, Page 1522
https://doi.org/10.1007/s12613-021-2306-2

Effect of Al_2O_3 content on the viscosity and structure of $CaO–SiO_2–Cr_2O_3–Al_2O_3$ slags

Fang Yuan, *Zheng Zhao*, *Yanling Zhang*✉, *and Tuo Wu*

State Key Laboratory of Advanced Metallurgy, University of Science and Technology Beijing, Beijing 100083, China
(Received: 4 January 2021; revised: 12 May 2021; accepted: 17 May 2021)

Abstract: The effect of Al_2O_3 content on the viscosity and structure of $CaO–SiO_2–Cr_2O_3–Al_2O_3$ slags was investigated to facilitate recycling of Cr in steelmaking slags. The slags exhibit good Newtonian behavior at high temperature. The viscosity of acidic slag first increases from 0.825 to 1.141 Pa·s as the Al_2O_3 content increases from 0 to 10wt% and then decreases to 1.071 Pa·s as the Al_2O_3 content increases further to 15wt%. The viscosity of basic slag first increases from 0.084 to 0.158 Pa·s as the Al_2O_3 content increases from 0 to 15wt% and then decreases to 0.135 Pa·s as the Al_2O_3 content increases further to 20wt%. Furthermore, Cr_2O_3-containing slag requires less Al_2O_3 to reach the maximum viscosity than Cr_2O_3-free slag; the Al_2O_3 contents at which the behavior changes are 10wt% and 15wt% for acidic and basic slags, respectively. The activation energy of the slags is consistent with the viscosity results. Raman spectra demonstrate that $[AlO_4]$ tetrahedra appear initially and were replaced by $[AlO_6]$ octahedra with further addition of Al_2O_3. The dissolved organic phosphorus content of the slag first increases and then decreases with increasing Al_2O_3 content, which is consistent with the viscosity and Raman results.

Keywords: viscosity; structure; Cr-containing slag; Raman spectra

1. Introduction

Viscosity is one of the important physicochemical property which significantly impacts the mass transfer of elements within the slag [1]. Knowing the viscosities of Cr-containing slag is essential for the metallurgical industry as Cr is in great demand and insufficient reserve in China [2]. However, researching progress about the viscosity of Cr-containing slags is slowly as following two difficult problems: firstly, it is proved that Cr can be oxidized easily and appears in two oxidation stages in metallurgical slags [3]: Cr^{2+} and Cr^{3+}. Secondly, the low solubility and high melting point of Cr_2O_3 always led to undissolved solid phase in silicate slag. The solid fraction increases with the decreasing temperature and the composition of the slag became more complex, which would also increase the solid fraction of the molten slag [4–5]. Many studies have demonstrated [3–5] that the valence states of Cr in molten slags, melting points, and solid fraction of molten slags were closely related with the temperature, oxygen potential, and the basicity of slag.

Nonetheless, the viscosity of different slag systems such as $CaO–SiO_2–MgO–x$wt%Cr_2O_3 slag, TiO_2-containing blast furnace slag, mold fluxes, $FeO–SiO_2–V_2O_3–TiO_2–Cr_2O_3$ slag, and alumina-rich slags have been measured by several researchers [6–17]. It can be seen that the highest temperature of these studies is below 1873 K (1600°C), moreover, complex components such as MgO, FeO, TiO_2 are containing in these slags. All these factors would lead to the increase of solid fraction of molten slag. The conclusions of the researches above showed that the slag viscosity of these research increases with increasing Cr_2O_3 content. It can be reasonably interpreted as the slag fluid measured by the above scholars containing many solid phases suspended in the slag such as $MgCr_2O_4$, $MgCrAlO_4$, $FeCr_2O_4$, and undissolved Cr_2O_3. With the increase of Cr_2O_3 content, the solid fraction of slag liquid increases and the increasing solid fraction leds to the increase of slag viscosity. Wu *et al.* [17] reported that Cr_2O_3 had a basic network-modifying character in $CaO–SiO_2–Al_2O_3$-based slag from 1953 to 1813 K and confirmed that the molten slag is homogeneous Newtonian fluid during the viscosity measurement, however, how the Al_2O_3 affects the viscosity of Cr-containing slag has not been studied.

Al_2O_3 can be used as a flux because of its ability to lower the melting point of slag. Further, the effect of Al_2O_3 on the structure of the slag has also been extensively studied [18–29]. Sohn and Min [25] found that Al_2O_3 is an amphoteric oxide. With increasing Al_2O_3 content, the Al_2O_3 transforms from acidic oxide to basic oxide and the behavior of Al_2O_3 changes from network former to network modifier. Park *et al.* [18–19] studied the effect of Al_2O_3 content on the viscosity of $CaO–SiO_2–(MgO)–Al_2O_3$ slag and concluded that with increasing Al_2O_3 content, the viscosity increased to a maximum value and then decreased, and its main reason is

✉ Corresponding author: Yanling Zhang E-mail: zhangyanling@metall.ustb.edu.cn

that the amphoteric behavior of Al_2O_3 in aluminosilicate melts.

Although Al_2O_3 strongly affects the fluidity of slag, its effect on the viscosity of Cr-containing slag is rarely reported. In addition, Cr^{3+}, like Al^{3+} in slags, is considered an amphoteric cation and can occupy both tetrahedral and octahedral sites [30]. However, the influence of Al^{3+} on the Cr-containing slag viscosity and the microstructure still remains to be researched.

In this study, the viscosity of $CaO–SiO_2–3wt\%Cr_2O_3–Al_2O_3$ [B = (mass ratio of CaO)/(mass ratio of SiO_2) = 0.5, 0.8, and 1.2] was measured by the rotating cylinder method at 1813–1953 K (1540–1680°C). Furthermore, the structure role of Al_2O_3 in the depolymerization and the polymerization of the silicate network was analyzed by applying Raman spectroscopy to the quenched slags.

2. Experimental

2.1. Calibration of viscometer

The schematic diagram of a high temperature viscometer is shown in Fig. 1, and the viscosity of Cr-containing slag was measured in cylinder rotation method. Before the measurement, a series of calibration operations should be carried out using the high temperature viscometer in order to accurately measure the viscosity of chromium slag.

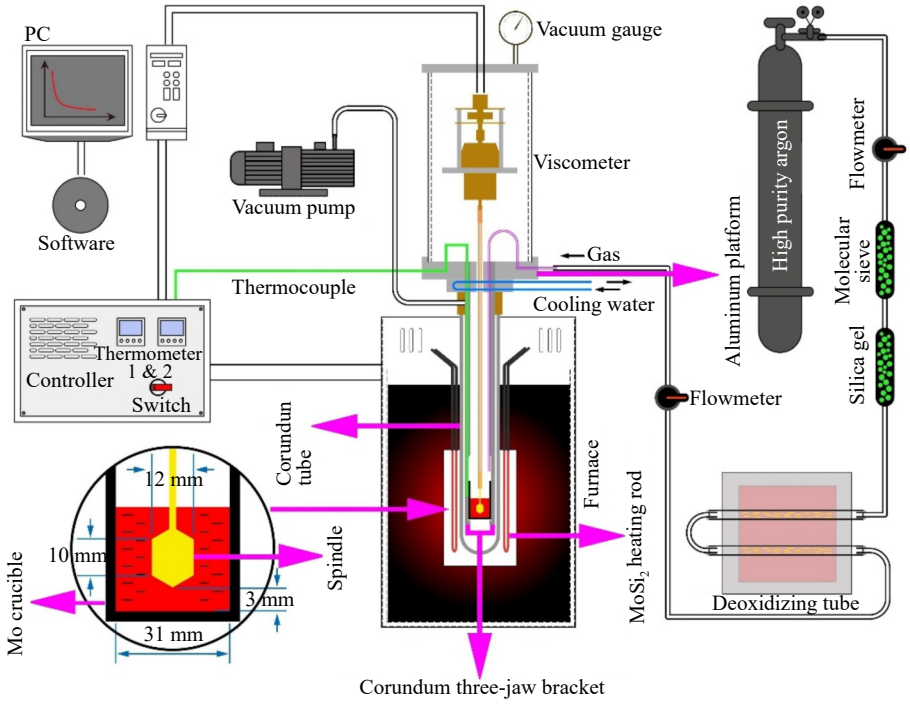

Fig. 1. Schematic diagram of experimental apparatus.

The first is the temperature calibration. The highest temperature of furnace used in this study can reach 1700°C which is suitable for measurements of Cr-containing slag with high melting point. As the viscosity of slag is very sensitive to temperature, the temperature of high temperature furnace must be properly controlled for the accuracy of the viscosity data. A single thermocouple (same with the furnace) is used to measure the temperature of different positions in the furnace in the temperature calibration and the temperature was compared with the temperature displayed by the controller, the results show that the constant temperature zone of the furnace is as high as 15 cm, and the temperature fluctuation in the constant temperature zone is ±2 K, which can meet the measurement accuracy conditions.

The second is the adjustment of the level. The spindle must be perpendicular to the horizontal line as the overall connection of the viscosity measurement system is flexible connection. Therefore, both the high temperature furnace and the placement platform of the viscometer must be horizontal to ensure that the spindle only revolve on its own axis during the measurement. The accuracy of viscosity was affected when the spindle has a certain swing in the slag and the slag viscosity will increase with the increasing amplitude of the swing according to the pre-experiment. Worse more, the spindle will knock against the crucible and damage the viscometer while the amplitude of the swing grows larger. Thus, the horizontal adjustment knob under the high temperature furnace and the horizontal adjustment screw of the platform should be adjusted to ensure that the spindle will not swing during the measurement.

Then there is the adjustment of coaxiality. The torque induced by viscometer comes from the shear flow field around the spindle and the inner wall of the crucible when the rotating spindle immersed in the melts. Therefore, whether the gap between the spindle and the inner wall of the crucible is well-distributed (the coaxiality of the spindle and the crucible) is particularly important to measure the accurate viscosity data. According to the pre-experiment, the deviation

between the center of the spindle and the center of the crucible will make the measured values higher, and the higher the viscosity of the slag is, the more obvious the effect is. We specially made a crucible cover with a hole (1 mm larger than the outer diameter of the spindle) in the center. The crucible cover was placed on the crucible before measurement and the platform descended slowly to make the spindle (at a rotation speed of 60 r/min) pass through the hole, then the coaxiality can be considered to meet the requirements.

The next step is to calibrate the viscometer. The viscosity measuring device used in this experiment is a cylinder rotary viscometer named Brookfield DV3T LV, whose constant parameter is called SMC (spindle multiplier constant) [31–32]. Generally, the constant can be determined by using one standard solution at the same speed. To ensure the accuracy of the constant, three kinds of silicone oil (100 cP, 500 cP, 5000 cP at 25°C, 1000 cP = 1 Pa·s) are used as the standard solution in this study, and three different rotation speeds are selected for viscosity measurement of each standard solution. Finally, the average value is taken as the final constant.

Finally, the experimental atmosphere needs to be controlled. A high purity molybdenum is used as the material of crucible and spindle in the measurement and Mo is easy to be oxidized, which makes the surface of crucible or spindle not smooth enough and leads to high viscosity. What's more, as a variable valence metal, Cr is also sensitive to oxygen partial pressure in atmosphere. Thus, all gases used in this experiment are high purity argon. In order to ensure the high purity of the gas, the secondary dehydration (molecular sieve and color changing silica gel) and secondary deoxidation (Pd deoxidizer) are needed, so that the O_2 and H_2O in the gas are less than 1.0 and 1.5 ppm respectively

2.2. Preparation of samples

The required reagent is pretreated (shown in Table 1) to remove the H_2O and CO_2. At the same time, the volume of the required slag was inferred combined with the size of the crucible, and the total weight of the required slag was calculated as 45 g by the estimated density of molten slags. The target slag composition of samples was shown in Table 2 and chosen in the phase diagram of $CaO–SiO_2–Cr_2O_3–Al_2O_3$ slags at 1873 K (shown in Fig. 2).

Table 1. Raw materials used for experiments

Material	Purity	Pretreatment	Provider
$CaCO_3$	≥99.0%	Decomposed at 1473 K for 12 h, verified by X-ray diffraction	Sinopharm Chemical Reagent Co., Ltd.
SiO_2	AR	Dried at 1073 K for 8 h	Sinopharm Chemical Reagent Co., Ltd.
Al_2O_3	AR	Dried at 1073 K for 8 h	Sinopharm Chemical Reagent Co., Ltd.
Cr_2O_3	≥99.0%	Dried at 1073 K for 8 h	Sinopharm Chemical Reagent Co., Ltd.
Mo	≥99.7%	Crucible and spindle were machined by CNC machine, deviation: ±0.02 mm	Baoji Sheng Hua Non-ferrous Materials Co., Ltd., China
Ar	≥99.999%	Dehydrated by molecular sieve and silica gel, deoxidized by Cu pieces (5 N) and Mg stripes (>99wt%) at 773 K	Beijing Qianxi gas company, China

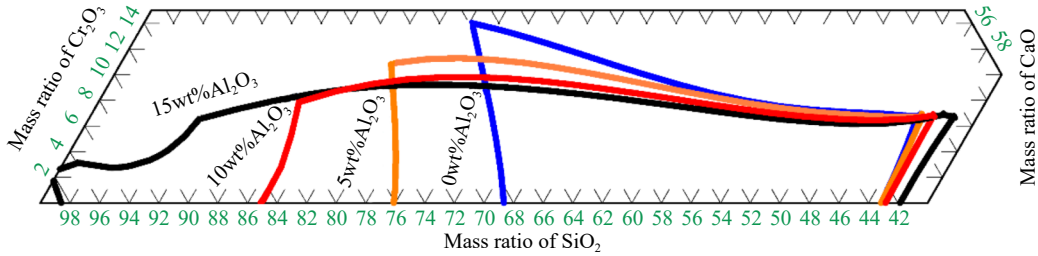

Fig. 2. Phase diagram of $CaO–SiO_2–Cr_2O_3$-based slags at 1873 K and effect of Al_2O_3 content on liquid regions.

2.3. Viscosity measurement

The spindle was removed and the viscometer was mechanically calibrated before the experiment. After that, the high temperature furnace and the viscometer were connected and sealed to form a closed system. Next, the vacuum pump was used to reduce the vacuum degree of the system to 10^{-2} atm and then start ventilation. The argon flow rate is set at 0.2 L/min when the air pressure returns to 1 atm and the flow speed is kept at 0.2 L/min until the end of the experiment.

The viscosity was measured by constant temperature method and the measurement was carried out every 10 K during the cooling process from 1953 to 1813 K. First, the furnace temperature is raised to 1953 K, and then the viscosity is measured every half hour. It is considered that the composition of the slag is homogeneous and the viscosity measurement can be started when the deviation of two consecutive measurements is ± 0.005 Pa·s. Then start to cool down at 3 K/min to the target temperature and keep for 1 h. Then the slag viscosity was measured with three different rotation speeds and the data was recorded. The torque of viscometer is set to 30%, 45%, and 60%, which are respectively recorded as rotation speed 1, 2, and 3 when selecting the rotational speed. Repeat this procedure until the temperature drops to 1813 K and the viscosity measurement is finished. Raise the temperature again to 1953 K and keep the temperature until

Table 2. Composition of CaO–SiO_2–3wt%Cr_2O_3–Al_2O_3 slags

No.	Target composition / wt%					X-ray fluorescence analysis results / wt%				
	CaO	SiO_2	Al_2O_3	Cr_2O_3	B_{target}	CaO	SiO_2	Al_2O_3	Cr_2O_3	B_{final}
A1	32.3	64.7	0.0	3.0	0.50	33.3	64.0	0.0	2.6	0.52
A2	30.7	61.3	5.0	3.0	0.50	31.2	61.4	4.8	2.6	0.51
A3	29.0	58.0	10.0	3.0	0.50	29.8	58.2	9.3	2.7	0.51
A4	27.3	54.7	15.0	3.0	0.50	27.7	55.4	14.2	2.7	0.50
A5	25.7	51.3	20.0	3.0	0.50	25.7	52.1	19.4	2.8	0.49
B4	36.4	45.6	15.0	3.0	0.80	37.7	44.9	14.9	2.5	0.84
C1	52.9	44.1	0.0	3.0	1.20	53.0	44.6	0.0	2.4	1.19
C2	50.2	41.8	5.0	3.0	1.20	50.8	41.6	4.9	2.7	1.22
C3	47.5	39.5	10.0	3.0	1.20	48.2	39.3	9.7	2.8	1.23
C4	44.7	37.3	15.0	3.0	1.20	45.1	37.7	14.3	2.9	1.20
C5	42.0	35.0	20.0	3.0	1.20	42.3	36.0	18.9	2.8	1.18
C6	39.3	32.7	25.0	3.0	1.20	40.1	33.2	23.9	2.8	1.21

the slag composition is homogeneous. Finally, the crucible was taken out from the furnace and thrown in cold water quickly for quench samples.

3. Results and discussion

3.1. Reliability analysis of viscosity measurements

It is particularly important to know whether the Cr-containing slag is a Newtonian fluid during the viscosity measurement as Cr-containing slag has the characteristics of high melting point. In this study, three rotation speeds were applied at each temperature to measure the viscosity. Twenty stable viscosity values were recorded at each rotation speed to obtain the viscosity of the slag and the measurements were done with temperature interval of 10 K from 1953 to 1813 K. Finally, the average value was taken as the viscosity data. The results are shown in Fig. 3.

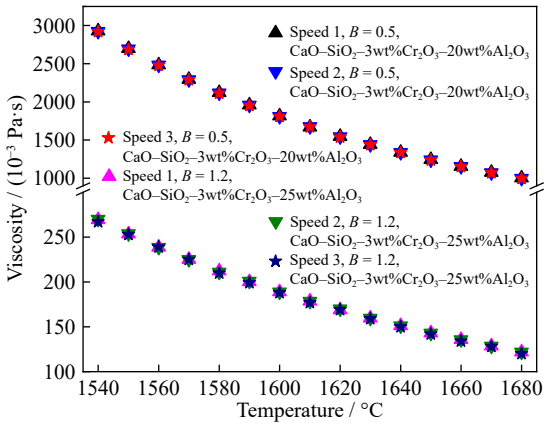

Fig. 3. Viscosity results of slags A5 and C6 at different rotation speeds.

At the highest alumina content, the viscosity of the slag at each rotation speed is almost the same even at the lowest temperature, and the relative deviation is no more than 2%. This also shows that the slag in this study acts as a Newtonian fluid, which is consistent with the results previously calculated by FactSage. Further, the slags were also confirmed to be in the glassy phase using X-ray diffraction (XRD) analysis, as shown in Fig. 4. In addition, the quenched samples with no characteristic peaks also meet the requirements of Raman spectroscopy.

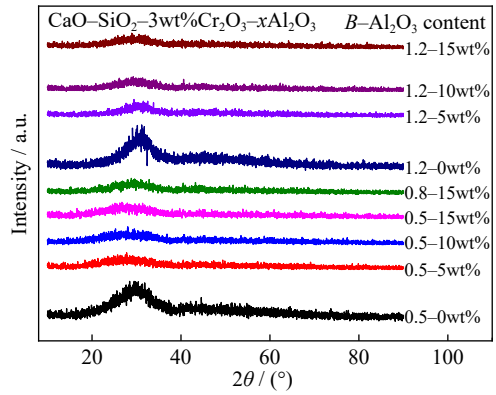

Fig. 4. XRD patterns of the quenched samples.

The results of the first and second viscosity measurements of some of the slags at 1953 K are compared in Table 3 to indicate the reproducibility of the viscosity measurements. The viscosity data of different slags at 1953 K are in good agreement. The relative deviations of the two measured viscosity data are less than 1.2%. Given the experimental uncertainties that are usually associated with viscosity measurements, the measurement methods adopted in this study are reliable.

3.2. Viscosity results

Fig. 5(a) shows the viscosity of the CaO–SiO_2–3wt%Cr_2O_3–Al_2O_3 (B = 0.5, 0.8, and 1.2) slags as a function of temperature. The slag viscosity generally decreased with increasing temperature and with increasing basicity. This main reason is that the amount of free oxygen (O^{2-}) dissociated from CaO increases [33], resulting in a decrease in the slag viscosity for B < 1.4, which is considered to have the lowest melting temperature among Cr-containing slags, according to Kalicka, Forsbacka, and Holappa and their co-authors [12,28,34]

Because Al_2O_3 is amphoteric, the effect of the Al_2O_3 content on the viscosity may depend on the basicity. The effect

Table 3. Reproducibility of viscosity measurement at 1953 K

No.	Viscosity / (10^{-3} Pa·s)						
	A1	A3	A5	B4	C1	C3	C5
1st	827.0	1145	1003	453.2	84.35	133.9	137.2
2nd	825.0	1141	1000	451.9	83.34	132.4	135.8
Relative deviation	0.242%	0.349%	0.299%	0.287%	1.197%	1.12%	1.02%

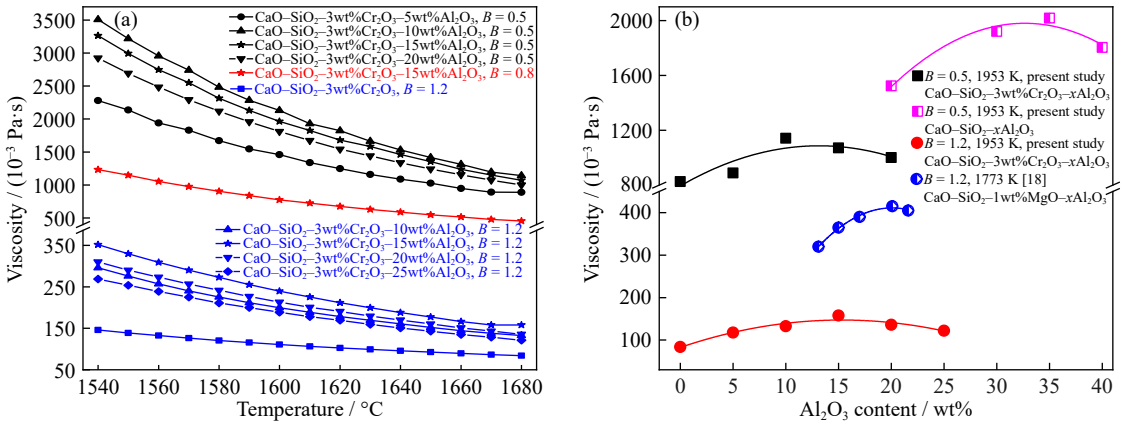

Fig. 5. (a) Temperature dependence of viscosity and (b) effect of Al_2O_3 content on slag viscosity.

of Al_2O_3 on the viscous behavior has been extensively studied [26–29,35–37]. It is generally believed that the viscosity of the slag first increases and then decreases with increasing Al_2O_3 content owing to its amphoteric behavior, which is consistent with the findings of the present study. Furthermore, Park *et al.* [18] studied the amphoteric behavior of Al_2O_3 in the CaO–SiO_2–MgO–Al_2O_3 slag system and found that with increasing Al_2O_3 content, the viscosity initially increases to the maximum at 21.6wt% and then decreases with further addition of Al_2O_3 when $B = 1.2$.

As shown in Fig. 5(b), the viscosity of Cr-containing slag with $B = 0.5$ first increased from 0.825 to 1.141 Pa·s as the Al_2O_3 content increased from 0 to 10wt% and then decreased to 1.071 Pa·s as the Al_2O_3 content was increased further to 15wt% at 1953 K. The viscosity of basic Cr-containing slag with $B = 1.2$ increased from 0.084 to 0.158 Pa·s as the Al_2O_3 content increased from 0 to 15wt% and then decreased to 0.135 Pa·s as the Al_2O_3 content was increased further to 20wt% at 1953 K.

The viscosity of Cr-free slags (CaO–SiO_2–(20wt%–40wt%) Al_2O_3 slag, measured in present study) and CaO–SiO_2–Al_2O_3–MgO slag measured by Park *et al.* [18] is also plotted here for comparison. The maximum viscosity is observed at approximately 35wt% of Al_2O_3 for the Cr-free slags when $B = 0.5$. The value becomes 21wt% when $B = 1.2$. The Al_2O_3 content required for maximum viscosity increased by 20% and 5% at $B = 0.5$ and 1.2, respectively, compared with that for Cr-containing slag. This result indicates that Cr_2O_3-containing slag requires less Al_2O_3 to reach the maximum viscosity than Cr_2O_3-free slag owing to the similarity in the structure and properties of Cr_2O_3 and Al_2O_3.

It is thought that [AlO_4] tetrahedra are the main structure of Al_2O_3 molecules when the viscosity is increased by adding Al_2O_3. With increasing Al_2O_3 content, the [AlO_4] tetrahedra began to change to [AlO_6] octahedra to substitute Ca^{2+}, as it can behave as a network modifier and reduce the slag viscosity. Considering that Cr^{3+}, like Al^{3+}, is an amphoteric cation in slags, [CrO_4] tetrahedra formed of Cr^{3+} will accelerate the change of [AlO_4] tetrahedra into [AlO_6] octahedra, reducing the Al_2O_3 content required for maximum viscosity.

3.3. Temperature dependence and activation energy of viscous flow

It is well known that temperature has an obvious effect on the viscosity of molten slag and the Arrhenius equation was used to describe the relationship between them [38]. The equation is shown as follow:

$$\ln \eta = \ln A + \frac{E_a}{R} \cdot \frac{1}{T} \tag{1}$$

where η is the slag viscosity (Pa·s), A is the pre-exponential factor, E_a is the activation energy (J·mol^{-1}), R is the gas constant (8.314 J·mol^{-1}·K^{-1}), and T is the temperature (K).

It can be seen from Eq. (1) that there is a linear relationship between lnη and 1/T. The corresponding viscosity data is substituted into the equation for linear fitting (shown in Fig. 6) and the linear correlation (R^2) of fitting equations is larger than 0.99 (shown in Table 4).

The activation energy (E_a) of viscous flow can be calculated from the fitting equations shown in Table 4 and the relationship between E_a and Al_2O_3 content is shown in Fig. 7. E_a of viscous flow is increased with increasing Al_2O_3 content until Al_2O_3 content reached 10wt% and 15wt% for acidic and basic slags, respectively. Then the increasing Al_2O_3 will decrease the E_a of viscous flow, which showed the same results with the viscosity measurement. In addition, increasing the basicity of slag in a certain range can effectively reduce the slag viscosity as the E_a of acid slag ($B = 0.5$) is significantly higher than that of basic slag ($B = 1.2$) under the same Al_2O_3

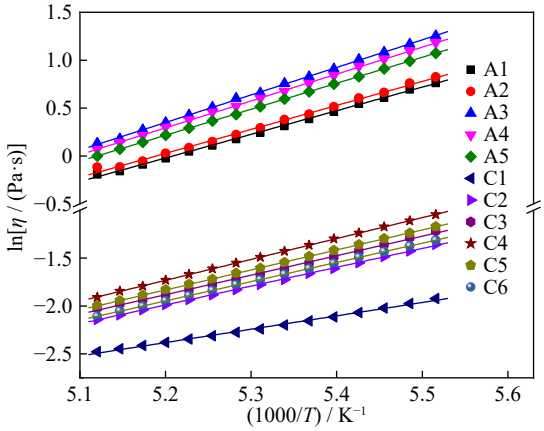

Fig. 6. Logarithm of viscosity versus reciprocal of temperature.

Table 4. Viscosity–temperature relationship

No.	ln *A*	E_a	R^2
A1	−12.847	205.06	0.996
A2	−12.976	207.90	0.992
A3	−14.599	239.00	0.998
A4	−14.296	233.27	0.999
A5	−13.899	225.68	0.999
C1	−9.633	115.93	0.994
C2	−12.204	163.33	0.998
C3	−12.464	169.19	0.999
C4	−13.074	181.34	0.997
C5	−12.692	173.63	1
C6	−12.400	167.13	0.999

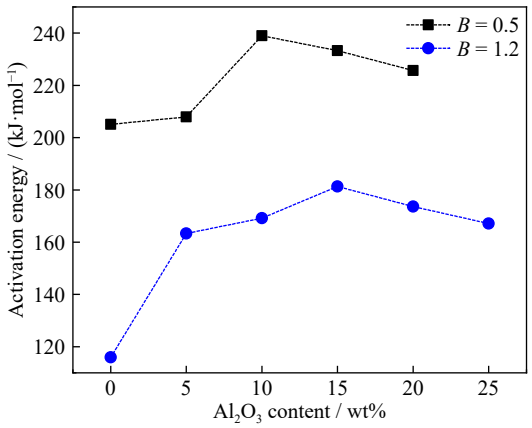

Fig. 7. Activation energy of viscous flow as a function of Al_2O_3 content.

content. The E_a of the slag represents the reduction of the minimum energy required for molecular migration in the slag. The higher the degree of slag polymerization, the higher the energy required, and the lower the degree of slag polymerization, the lower the energy required, which is also consistent with the experimental results.

3.4. Raman spectra of slag samples

It is common knowledge that the variation of slag microstructure units will affect the viscosity of molten slag [39] and the degree of polymerization (DOP) of molten slag is the main parameter to represent the microstructure units of molten slag. The study of slag microstructure mainly depends on Raman spectroscopy and the samples are required to be glassy slag for Raman spectrum detection. According to the XRD results shown in Fig. 4, the Raman results in this paper can be used to describe the change of slag microstructure units.

A lot of experience has been accumulated in the research of Raman spectroscopy [40] and the Raman spectrum of silicate can be divided into two different regions according to frequency. Different peak intensity in the low-frequency regions, from 400 to 800 cm^{-1}, represent the variation in the bridging oxygen (BO) bond content of I–O–I (I = Si, Ca, Al, Fe), and the changes of position in the high-frequency regions, from 800 to 1200 cm^{-1}, represent the content of Si–O–Si tetrahedral structural units (Q^n_{Si}). The Al–O^0 and Cr–O^0 bonds are weaker than the Si–O^0 bonds, as Al^{3+} and Cr^{3+} cations have a lower affinity toward O^{2-} anions than Si^{4+} cations do [41]. Therefore, the change in the tetrahedral [SiO_4] structure plays a dominant role in the slag structure.

Raman spectra of the $CaO–SiO_2–3wt\%Cr_2O_3–Al_2O_3$ (B = 0.5 and 1.2) system are presented in Fig. 8. As expected, it can be seen from the silica peak in the high frequency region of slag A that the [SiO_4] structure embedded with [AlO_4] increased gradually with the increase of Al_2O_3 content to 10wt%, the [SiO_4] area increased and the peak shifted to the right obviously. With the increase of Al_2O_3 content to 15wt%, [SiO_4] tetrahedra peaks of slag A4 became weaker than that of slag A3. When the basicity increases from 0.5 to 1.2, the [SiO_4] tetrahedra peaks are obviously moveout shifted leftward. This indicates that the number of bridging oxygens (BOs) in the [SiO_4] tetrahedra decreases gradually, and the structure tends to be simple, which is also consistent with the previous results on the effect of basicity on viscosity.

The symmetric stretching vibrations of Al–O–Al bonds appear at approximately 550 cm^{-1} [42], and the BOs of Al–O–Al increase gradually with increasing Al_2O_3 content. When B = 0.5, the [SiO_4] formed by the large amount of SiO_2 in the molten slag is the predominant unit and the [AlO_4] units cannot be observed as its extremely weak influence on [SiO_4]. The [AlO_6] octahedra peak appears at approximately

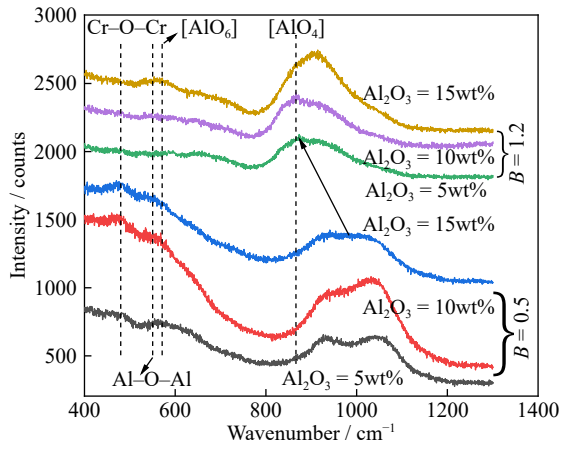

Fig. 8. Raman spectra of samples with different Al_2O_3 contents.

570 cm^{-1} [43] when the Al_2O_3 content is increased to 15wt%. This is particularly evident in the slag with $B = 1.2$. For Al_2O_3 contents of 5wt% and 10wt%, the $[AlO_4]$ peak was clearly present, whereas it was replaced by the $[AlO_6]$ peak when the Al_2O_3 content increased to 15wt%. This indicates that some of the structures of Al_2O_3 begin to change from $[AlO_4]$ to $[AlO_6]$ even though the slag viscosity continues to increase when the Al_2O_3 content increases to 15wt%. Like $[FeO_6]$, octahedral $[AlO_6]$ units would act as a network modifier in slag and reduce the slag viscosity, owing to its similar structure. It can be inferred that more $[AlO_6]$ will form with further addition of Al_2O_3 and lead to the decrease in slag viscosity, which is also similar to the results of Park's studies [29].

In general, Cr–O–Cr bonds will be formed in the low frequency region of Raman spectrum of Cr_2O_3-containing slag and the microstructure unit will be assigned to the Raman band at 439 cm^{-1} [44–45]. However, the peaks representing $[CrO_6]$ octahedra and $[CrO_4]$ tetrahedra, which typically appear at approximately 700 and 850 cm^{-1} [43], are not observed in the present experiment, as shown in Fig. 8, possibly because of the low chromium content (3wt%).

Frantza and Mysen [46] reported that the Raman spectra of silicate can be deconvoluted with Gaussian deconvolution method to accurately describe the structural characteristics of silicate and other related details. In addition, the corresponding positions of different silicate structures in the high-frequency region are shown in Table 5 and the BO numbers of corresponding structure unit are also listed.

Table 5. Specific characteristics of Q^n_{Si}

Raman shift / cm^{-1}	Units	Raman assignment
850–880	SiO_4^{4-}	With zero bridging oxygen in a monomer structure (Q^0_{Si})
900–920	$Si_2O_7^{6-}$	With one bridging oxygen in dimer structure unit (Q^1_{Si})
950–980	$Si_2O_6^{4-}$	With two bridging oxygen in chain structure unit (Q^2_{Si})
1040–1100	$Si_2O_5^{2-}$	With one bridging oxygen in sheet structure unit (Q^3_{Si})
1060, 1190	SiO_2	With four BO atoms in a network

Generally, the relative Raman peak area (A_i) is linearly related to its corresponding content of Q^n_{Si} and the relationship between Raman peak area fraction and mole fraction of structural units can be calculated using Eq. (2).

$$Q_i = \frac{A_i}{(A_0 + A_1 + A_2 + A_3 + A_4)} \tag{2}$$

However, the Q^n_{Si} content cannot be simply expressed by the Raman peak area fraction, although there is a linear relationship between them. Raman scattering coefficient (θ) is also closely related to it and the Raman scattering coefficient of species i (θ_i) can be got from the Raman scattering cross section of the vibration mode [47]. The relationship between the mole fractions of structural units (X_i) and the relative areas of each deconvoluted band (A_i) are shown as Eq. (3) according to Frantza and Mysen [46].

$$X_i = \theta_i A_i,\ i = 0, 1, 2, \text{ and } 3 \tag{3}$$

However, as the absolute Raman intensity is an inaccessible data, the Raman scattering coefficient can only be obtained as a relative value or in the simulation calculation method. Wu *et al.* [48] assumed five values from S_0 to S_4 and the values got through simulation calculation method are consistent with the results obtained by other researchers from quantitative analyses of experimental spectra [49–51].

Therefore, Eqs. (2) and (3) should be integrated into Eq. (4) with the aforementioned theory basis for the calculation of the mole fractions of structural units, the equation is shown as follows and the values of S_i are obtained from Wu *et al.* [48].

$$X_i = \frac{A_i/S_i}{\sum_{i=0}^{4} A_i/S_i} \tag{4}$$

The Raman spectra of the $CaO–SiO_2–3wt\%Cr_2O_3–Al_2O_3$ ($B = 0.5$ and 1.2) slags were deconvoluted and the deconvolution results are shown in Fig. 9(a–c); the minimum correlation coefficient R^2 was 0.998. The structural units of slag A are shown in Fig. 9(d).

As shown, the Q^3_{Si} and Q^4_{Si} contents obviously increase as the $A1_2O_3$ content increases from 5wt% to 10wt%, whereas the Q^1_{Si} content decreases, indicating that the $[SiO_4]$ tetrahedra will be more polymerized and robust and will limit the fluidity of the slag. As the Al_2O_3 content increases further to 15wt%, the Q^3_{Si} and Q^4_{Si} contents decrease; by contrast, the Q^1_{Si} content increases, and the slag viscosity decreases, facilitating mass transfer and slag–alloy separation. It is thought that the $[AlO_4]$ tetrahedra were formed by the Al_2O_3 molecules and the molten slag when Al_2O_3 is added to increase the viscosity. With increasing Al_2O_3 content, the $[AlO_4]$ tetrahedra begin to change to $[AlO_6]$ octahedra to substitute Ca^{2+}, as they can behave as a network modifier and reduce the slag viscosity. This is also consistent with the analysis results in the low-frequency region.

NBO/Si, the average number of non-bridging oxygen atoms on a Si atom, is used to describe the degree of polymerization of slag. The DOP of slag decreases with the increase of NBO/Si. The NBO/Si of samples in current study can be calculated by Eq. (4) according to the mole fractions of the structural units above.

$$\text{NBO/Si} = \sum_{i=0}^{4} (1 - X_i) \tag{5}$$

Fig. 10 shows the effect of Al_2O_3 on the NBO/Si values calculated from the Raman spectra. The NBO/Si of the slag A first decreases with the increasing Al_2O_3 content from 0 to

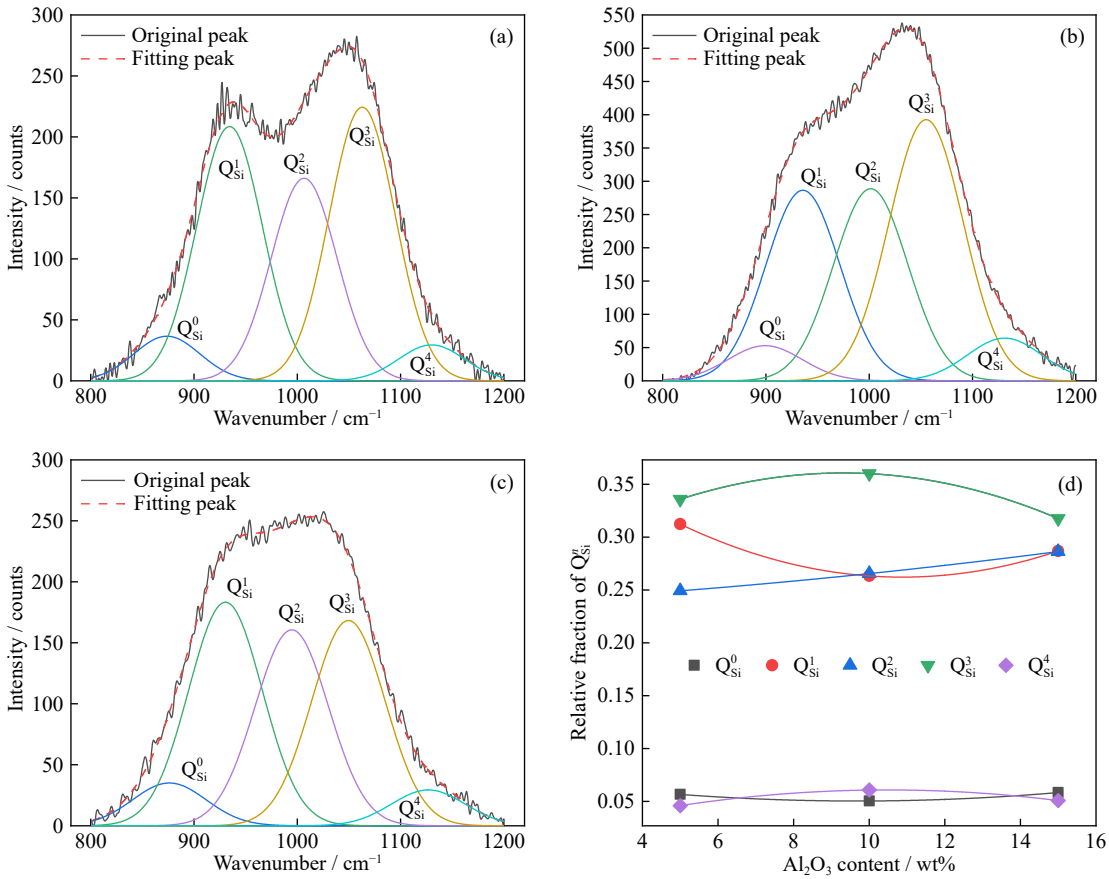

Fig. 9. Deconvoluted Raman spectra of slags (a) A1, (b) A2, and (c) A3. (d) Structural units of slag A.

10wt%, and then increases with continuous addition of Al_2O_3 to 15wt%, the molten slag first polymerized and then disassembled, which showing no difference with the viscosity measurements. What's more, the NBO/Si decreases gradually with increasing Al_2O_3 content from 0 to 15wt% and these results show that the silicate networks become more complex for slag C, which is also consistent with the viscosity results. It can be inferred from the calculation results that the DOP of slags corresponds to its viscosity.

The structural changes can be reasonably explained as the viscosity and Raman analyses in this study revealed amphoteric behavior of Al^{3+}. Generally, Ca^{2+} appeared near $[AlO_4]$ tetrahedra and $[SiO_4]$ tetrahedra as both a charge compensator and a network modifier. According to the results of Raman spectra, Ca^{2+} ions can hardly completely supply for slags with a high Al_2O_3 content owing to the scarcity of Ca^{2+} as the Al_2O_3 content increases to 15wt%. Under this condition, the $[AlO_4]$ tetrahedra begin to change to $[AlO_6]$ octahedra to substitute Ca^{2+}, as they can behave as a network modifier and reduce the slag viscosity, which facilitates mass transfer and slag–alloy separation in the melting process and increase the Cr yield.

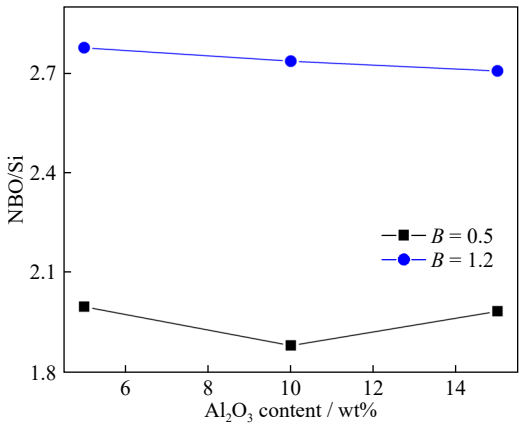

Fig. 10. Effect of Al_2O_3 content on NBO/Si.

4. Conclusion

$CaO–SiO_2–Cr_2O_3–Al_2O_3$ slags showed good Newtonian behavior at high temperatures, and the viscosity of the $CaO–SiO_2–3wt\%Cr_2O_3–x\%Al_2O_3$ slags first increased with increasing Al_2O_3 content and then decreased as the Al_2O_3 content increased further at 1953 K for B = 0.5 and 1.2. Furthermore, Cr_2O_3-containing slags required less Al_2O_3 to reach the maximum viscosity than Cr_2O_3-free slag. The activation energy of the slags viscous flow increased at first and decreased afterwards with increasing Al_2O_3 content. Al_2O_3 contents at which the behavior changed were 10wt% and 15wt% for acidic and basic slags, respectively. Raman spectra of the slags showed that the number of Al–O–Al bonds increases gradually with increasing Al_2O_3 content. $[AlO_4]$ tetrahedra were observed initially and then were replaced by $[AlO_6]$ octahedra with further addition of Al_2O_3. This also explained why the slag viscosity increased at first and decreased after-

wards with increasing Al_2O_3 content. The deconvoluted Raman spectra showed that with increasing Al_2O_3 content, the Q^3_{Si} and Q^4_{Si} contents obviously increase and then decrease, whereas the Q^1_{Si} content first decreases and then increases. The DOP content of the slags first increases and then decreases with increasing Al_2O_3 content, which is consistent with the viscosity and Raman results.

Acknowledgements

This work was financially supported by the National Natural Science Foundation of China (No. U1960201) and the National Key R&D Program of China (No. 2019YFC 1905701).

Conflict of Interest

The authors declare no potential conflicts of interest.

References

[1] K.I. Miyamoto, K. Kato, and T. Yuki, Effect of slag properties on reduction rate of chromium oxide in Cr_2O_3 containing slag by carbon in steel, *Tetsu-to-Hagane*, 88(2002), No. 12, p. 838.
[2] X.T. Zeng, C.H. Yuan, H. Xu, J.X. Han and Y. Tian, Development status quo of the world chromite resources and investment suggestion, *China Min.*, 24(2015), No. 8, p. 16.
[3] M. Kekkonen, H. Oghbasilasie, and S. Louhenkilpi, *Viscosity Models for Molten Slags*, Aalto University publication series, Helsinki, 2012.
[4] L.J. Wang and S. Seetharaman, Experimental studies on the oxidation states of chromium oxides in slag systems, *Metall. Mater. Trans. B*, 41(2010), No. 5, p. 946.
[5] V.D. Eisenhüttenleute, *Slag Atlas*, 2nd ed., Verlag Stahleisen GmbH, Düsseldorf, 1995.
[6] E. Minami, M. Amatatsu, and N. Sano, Viscosity measurement of slag containing chromium oxide, *Tetsu-to-Hagane*, 73(1987), p. S871.
[7] G.B. Qiu, L. Chen, J.Y. Zhu, X.W. Lv, and C.G. Bai, Effect of Cr_2O_3 addition on viscosity and structure of Ti-bearing blast furnace slag, *ISIJ Int.*, 55(2015), No. 7, p. 1367.
[8] C. Xu, W.L. Wang, L.J. Zhou, S.L. Xie, and C. Zhang, The effects of Cr_2O_3 on the melting, viscosity, heat transfer, and crystallization behaviors of mold flux used for the casting of Cr-bearing alloy steels, *Metall. Mater. Trans. B*, 46(2015), No. 2, p. 882.
[9] W.J. Huang, Y.H. Zhao, S. Yu, L.X. Zhang, Z.C. Ye, N. Wang, and M. Chen, Viscosity property and structure analysis of $FeO–SiO_2–V_2O_3–TiO_2–Cr_2O_3$ slags, *ISIJ Int.*, 56(2016), No. 4, p. 594.
[10] R.Z. Xu, J.L. Zhang, Z.Y. Wang, and K.X. Jiao, Influence of Cr_2O_3 and B_2O_3 on viscosity and structure of high alumina slag, *Steel Res. Int.*, 88(2017), No. 4, art. No. 1600241.
[11] Q.H. Li, J.T. Gao, Y.L. Zhang, Z.Q. An, and Z.C. Guo, Viscosity measurement and structure analysis of Cr_2O_3-bearing $CaO–SiO_2–MgO–Al_2O_3$ slags, *Metall. Mater. Trans. B*, 48(2017), No. 1, p. 346.
[12] L. Forsbacka, and L. Holappa, Viscosity of $SiO_2–CaO–CrO_x$ slags in contact with metallic chromium and application of the Iida model, [in] *VII International Conference on Molten Slags, Fluxes and Salts*, Johannesburg, 2004, p. 129.
[13] L. Forsbacka, L. Holappa, A. Kondratiev, and E. Jak, Experimental study and modelling of viscosity of chromium containing slags, *Steel Res. Int.*, 78(2007), No. 9, p. 676.
[14] L. Forsbacka and L. Holappa, Viscosity of $CaO–CrO_x–SiO_2$ slags in a relatively high oxygen partial pressure atmosphere, *Scand. J. Metall.*, 33(2004), No. 5, p. 676.
[15] K.C. Mills, L. Yuan, Z. Li, G.H. Zhang, and K.C. Chou, A review of the factors affecting the thermophysical properties of silicate slags, *High Temp. Mater. Processes*, 31(2012), No. 4-5, p. 301.
[16] F. Yuan, Z. Zhao, Y.L. Zhang, J.T. Gao, and T. Wu, Viscosity measurements of CrO-bearing $CaO–SiO_2–5\%Al_2O_3–CrO$ slag equilibrating with metallic Cr, *ISIJ Int.*, 60(2020), No. 3, p. 613.
[17] T. Wu, Y.L. Zhang, F. Yuan, and Z.Q. An, Effects of the Cr_2O_3 content on the viscosity of $CaO–SiO_2–10Pct\ Al_2O_3–Cr_2O_3$ quaternary slag, *Metall. Mater. Trans. B*, 49(2018), No. 4, p. 1719.
[18] J.H. Park, H. Kim, and D.J. Min, Novel approach to link between viscosity and structure of silicate melts via Darken's excess stability function: Focus on the amphoteric behavior of alumina, *Metall. Mater. Trans. B*, 39(2008), No. 1, p. 150.
[19] J.H. Park, D.J. Min, and H.S. Song, Amphoteric behavior of alumina in viscous flow and structure of $CaO–SiO_2$ (–MgO) $–Al_2O_3$ slags, *Metall. Mater. Trans. B*, 35(2004), No. 2, p. 269.
[20] F. Shahbazian, S.C. Du, and S. Seetharaman, The effect of addition of Al_2O_3 on the viscosity of CaO–"FeO"–SiO_2–CaF_2 slags, *ISIJ Int.*, 42(2002), No. 2, p. 155.
[21] H.S. Park, S.S. Park, and I. Sohn, The viscous behavior of $FeO_t–Al_2O_3–SiO_2$ copper smelting slags, *Metall. Mater. Trans. B*, 42(2011), No. 4, p. 692.
[22] B.O. Mysen, D. Virgo, and C.M. Scarfe, Relations between the anionic structure and viscosity of silicate melts—A Raman spectroscopic study, *Am. Mineral.*, 65(1980), No. 7-8, p. 690.
[23] P. McMillan, A Raman spectroscopic study of glasses in the system $CaO–MgO–SiO_2$, *Am. Mineral.*, 69(1984), No. 7-8, p. 645.
[24] D.R. Neuville, L. Cormier, and D. Massiot, Al coordination and speciation in calcium aluminosilicate glasses: Effects of composition determined by 27Al MQ-MAS NMR and Raman spectroscopy, *Chem. Geol.*, 229(2006), No. 1-3, p. 173.
[25] I. Sohn and D.J. Min, A review of the relationship between viscosity and the structure of calcium-silicate-based slags in ironmaking, *Steel Res. Int.*, 83(2012), No. 7, p. 611.
[26] C.Y. Xu, C. Wang, R.Z. Xu, J.L. Zhang, and K.X. Jiao, Effect of Al_2O_3 on the viscosity of $CaO–SiO_2–Al_2O_3–MgO–Cr_2O_3$ slags, *Int. J. Miner. Metall. Mater.*, 28(2021), No. 5, p. 797.
[27] K.Z. Gu, W.L. Wang, J. Wei, H. Matsuura, F. Tsukihashi, I. Sohn, and D.J. Min, Heat-transfer phenomena across mold flux by using the inferred emitter technique, *Metall. Mater. Trans. B*, 43(2012), No. 6, p. 1393.
[28] L. Forsbacka, L. Holappa, T. Iida, Y. Kita, and Y. Toda, Experimental study of viscosities of selected $CaO–MgO–Al_2O_3–SiO_2$ slags and application of the Iida model, *Scand. J. Metall.*, 32(2003), No. 5, p. 273.
[29] J.R. Kim, Y.S. Lee, D.J. Min, S.M. Jung, and S.H. Yi, Influence of MgO and Al_2O_3 contents on viscosity of blast furnace type slags containing FeO, *ISIJ Int.*, 44(2004), No. 8, p. 1291.
[30] Y.B. Cheng, C. Xu, S.Y. Pan, Y.F. Xia, R.C. Liu, and S.X. Wang, An investigation of the structural effects of Fe^{3+} in the alkali-silicate glasses, *J. Non-Cryst. Solids*, 80(1986), No. 1-3, p. 201.
[31] L. Forsbacka, *Experiences in Slag Viscosity Measurement by Rotation Cylinder Method*, Helsinki University of Technology, Helsinki, 2015.
[32] M. Chen, S. Raghunath, and B.J. Zhao, Viscosity of SiO_2–"FeO"–Al_2O_3 system in equilibrium with metallic Fe, *Metall. Mater. Trans. B*, 44(2013), No. 4, p. 820.
[33] J.H. Park, Composition–structure–property relationships of $CaO–MO–SiO_2$ (M = Mg^{2+}, Mn^{2+}) systems derived from micro-Raman spectroscopy, *J. Non Cryst. Solids*, 358(2012), No. 23,

p. 3096.
[34] Z. Kalicka, E. Kawecka-Cebula, and K. Pytel, Application of the Iida model for estimation of slag viscosity for $Al_2O_3–Cr_2O_3–CaO–CaF_2$ systems, *Arch. Metall. Mater.*, 54(2009), No. 1, p. 179.
[35] J.F. Lü, Z.N. Jin, H.Y. Yang, L.L. Tong, G.B. Chen, and F.X. Xiao, Effect of the CaO/SiO_2 mass ratio and FeO content on the viscosity of $CaO–SiO_2$–"FeO"–12wt%ZnO–3wt%Al_2O_3 slags, *Int. J. Miner. Metall. Mater.*, 24(2017), No. 7, p. 756.
[36] C.B. Shi, D.L. Zheng, S.H. Shin, J. Li, and J.W. Cho, Effect of TiO_2 on the viscosity and structure of low-fluoride slag used for electroslag remelting of Ti-containing steels, *Int. J. Miner. Metall. Mater.*, 24(2017), No. 1, p. 18.
[37] J.S. Machin, T.B. Yee, and D.L. Hanna, Viscosity studies of system $CaO–MgO–Al_2O_3–SiO_2$: III, 35, 45, and 50% SiO_2, *J. Am. Ceram. Soc.*, 35(1952), No. 12, p. 322.
[38] S. Arrhenius, The viscosity of aqueous mixture, *Z. Phys. Chem.*, 1(1887), p. 285.
[39] K.C. Mills, The influence of structure on the physico-chemical properties of slags, *ISIJ Int.*, 33(1993), No. 1, p. 148.
[40] G.C. Jiang and J.L. You, High temperature Raman spectroscopy used in the study of microstructure of silicate melts, *J. Chin. Ceram. Soc.*, 31(2003), No. 10, p. 998.
[41] R.D. Shannon, Revised effective ionic radii and systematic studies of interatomic distances in halides and chalcogenides, *Acta Crystallogr. Sect. A*, 32(1976), No. 5, p. 751.
[42] T.S. Kim and J.H. Park, Structure–viscosity relationship of low-silica calcium aluminosilicate melts, *ISIJ Int.*, 54(2014), No. 9, p. 2031.
[43] L.J. Wang, Y.X. Wang, Q. Wang, and K. Chou, Raman structure investigations of $CaO–MgO–Al_2O_3–SiO_2–CrO_x$ and its correlation with sulfide capacity, *Metall. Mater. Trans. B*, 47(2016), No. 1, p. 10.
[44] T.J. Dines and S. Inglis, Raman spectroscopic study of supported chromium(VI) oxide catalysts, *Phys. Chem. Chem. Phys.*, 5(2003), No. 6, p. 1320.
[45] J.J. Yang, H.F. Cheng, W.N. Martens, and R.L. Frost, Transition of synthetic chromium oxide gel to crystalline chromium oxide: A hot-stage Raman spectroscopic study, *J. Raman Spectrosc.*, 42(2011), No. 5, p. 1069.
[46] J.D. Frantza and B.O. Mysen, Raman spectra and structure of $BaO–SiO_2–SrO–SiO_2$ and $CaO–SiO_2$ melts to 1600°C, *Chem. Geol.*, 121(1995), No. 1-4, p. 155.
[47] B.O. Mysen and J.D. Frantz, Structure of silicate melts at high temperature: *In-situ* measurements in the system $BaO–SiO_2$ to 1669°C, *Am. Mineral.*, 78(1993), No. 7-8, p. 699.
[48] Y.Q. Wu, G.C. Jiang, J.L. You, H.Y. Hou, and H. Chen, Raman scattering coefficients of symmetrical stretching modes of microstructural units in sodium silicate melts, *Acta Phys. Sin.*, 54(2005), No. 2, art. No. 961.
[49] B.O. Mysen and J.D. Frantz, Silicate melts at magmatic temperatures: *In-situ* structure determination to 1651°C and effect of temperature and bulk composition on the mixing behavior of structural units, *Contrib. Mineral. Petrol.*, 117(1994), No. 1, p. 1.
[50] J.F. Stebbins, Effects of temperature and composition on silicate glass structure and dynamics: SI-29 NMR results, *J. Non-Cryst. Solids*, 106(1988), No. 1-3, p. 359.
[51] J.L. You, G.C. Jiang, and K.D. Xu, High temperature Raman spectra of sodium disilicate crystal, glass and its liquid, *J. Non-Cryst. Solids*, 282(2001), No. 1, p. 125.